Published in final edited form as:
Mol Cell. 2008 November 21; 32(4): 564–575. doi:10.1016/j.molcel.2008.09.022.

The Skap-hom Dimerization and PH Domains Comprise a 3′-Phosphoinositide-Gated Molecular Switch

Kenneth D. Swanson[1,*], **Yong Tang**[2,3,*], **Derek F. Ceccarelli**[2,4], **Florence Poy**[2], **Jan P. Sliwa**[2], **Benjamin G. Neel**[1,5,†], and **Michael J. Eck**[2,†]

1 *Cancer Biology Program, Division of Hematology-Oncology, Department of Medicine, Beth Israel Deaconess Medical Center, Boston, MA 02115*

2 *Department of Cancer Biology, Dana-Farber Cancer Institute, and Department of Biological Chemistry and Molecular Pharmacology, Harvard Medical School, Boston, MA 02115*

Summary

PH domains, by binding to phosphoinositides, often serve as membrane-targeting modules. Using crystallographic, biochemical and cell biological approaches, we have uncovered a mechanism that the integrin-signaling adaptor Skap-hom uses to mediate cytoskeletal interactions. Skap-hom is a homodimer containing an N-terminal four-helix-bundle dimerization domain, against which its two PH domains pack in a conformation incompatible with phosphoinositide binding. The isolated PH domains bind PI[3,4,5]P_3, and mutations targeting the dimerization domain or the PH domain's PI[3,4,5]P_3-binding pocket prevent Skap-hom localization to ruffles. Targeting is retained when the PH domain is deleted or by combined mutation of the PI[3,4,5]P_3-binding pocket and the PH/dimerization domain interface. Thus, the dimerization and PH domain form a novel PI[3,4,5]P_3-responsive molecular switch that controls Skap-hom function.

Keywords

Skap55; Pleckstrin Homology Domain; Macrophages; Actin cytoskeleton; Crystal Structure

Introduction

Cells use a variety of modular domains and motifs to target signaling molecules appropriately. One common module, the Pleckstrin homology (PH) domain, is found in molecules as diverse as kinases, guanine nucleotide-exchange factors (GEFs), and adaptors. Some PH domains, including the PH domains of Btk, Akt and Grp1, exhibit high affinity binding to phosphoinositides. Consequently, the conventional view is that PH domains direct signaling

†Correspondence should be addressed to M.J.E at eck@red.dfci.harvard.edu or to B.G.N. at bneel@uhnresearch.ca.
*These authors contributed equally
3Current address: Program in Gene Expression and Regulation, The Wistar Institute, 3601 Spruce Street, Philadelphia, PA 19104
4Current address: Samuel Lunenfeld Research Institute, Mount Sinai Hospital, Toronto, Ontario, Canada M5G 1X5.
5Current address: Ontario Cancer Institute, Department of Medical Biophysics, University of Toronto, Toronto, Ontario, Canada M5G 1L7

Competing Interest Statement
The authors declare that they have no competing financial interests.

components to sites of phosphoinositide production on various cellular membranes. But a comprehensive survey has shown that most PH/phosphoinositide interactions are relatively weak, implying that PH domains may have additional functions (Lemmon, 2004). Some PH domains do bind specific proteins (Lemmon, 2004), and recently, the SOS1 PH domain was reported to bind phosphatadic acid (Zhao et al., 2007). Yet the biochemical and physiological functions of the majority of PH domains remain unknown.

Adaptors function downstream of receptors, including those for growth factors, cytokines, antigens and cell adhesion molecules, and primarily consist of domains that mediate protein/protein and/or protein/membrane interactions (Simeoni et al., 2004). Some adaptors help reorganize the cytoskeleton and/or promote integrin-mediated adhesion upon immunoreceptor activation. In T lymphocytes, these include Adap (adhesion and degranulation promoting adaptor protein, previously known as Fyn-binding protein, Fyb) (da Silva et al., 1997; Griffiths et al., 2001; Peterson et al., 2001) and its binding partner Skap55 (Src-kinase-associated phosphoprotein of 55 kDa) (Wang et al., 2003). Adap55$^{-/-}$ T cells fail to activate the integrin Lfa-1 in response to T cell receptor (TCR) stimulation, and have severe functional defects (Griffiths et al., 2001; Peterson et al., 2001). Skap55$^{-/-}$ T cells have a similar phenotype (Wang et al., 2007), suggesting that Skap55 and Adap act together to promote integrin activation. Exactly how this occurs remains unclear. Adap binds Vasp and Wasp, suggesting a role in Arp2/3 recruitment and *de novo* actin polymerization (Coppolino et al., 2001; Krause et al., 2000). Skap55 has a previously uncharacterized N-terminal region, a central PH domain, a C-terminal SH3 domain that binds Adap, and intervening linkers with tyrosine phosphorylation sites. Given these features, Skap55 might function to target Adap in response to TCR activation, in which case the Skap55$^{-/-}$ phenotype would reflect effective Adap deficiency. Alternatively, because Adap stabilizes Skap55 (Huang et al., 2005), the Adap$^{-/-}$ phenotype could be due to effective Skap55 deficiency. On the other hand, recent data indicate that the Skap55/Adap complex binds Riam1 (Kliche et al., 2006; Menasche et al., 2007), a Rap1 effector that recruits and stimulates the integrin-activating protein Talin (Wegener et al., 2007). Skap55 and Adap alone lack this function, suggesting that a novel Riam1-binding surface is generated or exposed in the Skap55/Adap complex.

Adap is expressed broadly in lympho-hematopoietic cells (da Silva et al., 1997), but Skap55 is expressed solely in T lymphocytes (Marie-Cardine et al., 1997). The concerted actions of Skap55 and Adap suggest that another protein(s) substitutes for Skap55 in, for example, myeloid cells. Skap-hom (Skap55 homolog), has the same architecture as Skap55 (Figure 1A), and is expressed widely in lympho-hematopoietic cells (Curtis et al., 2000; Kouroku et al., 1998; Marie-Cardine et al., 1998). Skap-hom also associates via its SH3 domain with Adap, and is implicated in integrin signaling. For example, Skap-hom interacts with actin (Bourette et al., 2005) and, with Adap, undergoes tyrosine phosphorylation in response to plating of bone marrow-derived macrophages (BMM) on fibronectin (Timms et al., 1999). Skap-hom and Adap are substrates for the virulence factor YopH, a tyrosine phosphatase encoded by enteropathogenic *Yersinia* species and dephosphorylation of Skap-hom appears to interfere with adhesion-dependent events in phagocytosis (Black et al., 2000; Fallman et al., 2002). Finally, Skap-hom$^{-/-}$ B cells show defective adhesion in response to B cell receptor stimulation (Togni et al., 2005).

Although Skap proteins couple receptors to cytoskeletal rearrangements, their biochemical properties and mechanism of action remain poorly understood. For example, whether Skap PH domains bind phosphoinositides, and if so which ones, has not been determined. The sequence of the N-terminus of Skap-hom suggests a coiled-coil oligomerization element (Marie-Cardine et al., 1998), but it is unclear whether Skap55 and Skap-hom multimerize *in vivo*.

To provide a foundation for dissecting the function and regulation of SKAP proteins, we undertook a structural and biochemical analysis of Skap-hom. Our results reveal an unusual four-helix-bundle dimerization domain in the Skap-hom N-terminus, and show that the dimerization and PH domains comprise a PI[3,4,5]P3-sensitive conformational switch that regulates its sub-cellular targeting.

Results

The Skap-hom DM-PH region forms a dimer

Besides their well-defined PH and SH3 domains, Skap proteins have a region of homology in their N-termini suggesting an as yet undefined structural domain (Figures 1A, B). Bioinformatic analysis had suggested that in Skap-hom (but not Skap55), this region adopts a coiled-coil conformation (Marie-Cardine et al., 1998). To test this prediction, we prepared murine Skap-hom fragments containing the N-terminal and PH domains (residues 14–222; termed DM-PH as noted below) or the isolated PH domain (residues 101–222). Size-exclusion chromatography and dynamic light scattering showed that the isolated PH domain was monomeric, but the DM-PH fragment formed a dimer (Supplementary Figure 1, Supplementary Table 1).

Overall structure—We crystallized and solved the structure of the DM-PH fragment at a resolution of 2.6 Å (Table 1) with a crystallographic R factor of 17.9% (R_{free}=21.6%). The protein crystallized in space group C2 with two molecules per asymmetric unit and, consistent with its behavior in solution, formed a dimer (Figure 1C). Dimer formation is mediated by helical segments in the N-terminal region, with two helices from each polypeptide chain packing together via extensive hydrophobic interactions to form a 4-helix bundle, hereafter termed the dimerization (DM) domain. The two PH domains flank the 4-helix bundle and show the characteristic PH domain fold, consisting of a β-sandwich capped on one end by a C-terminal α-helix (Figure 1C; see also Figures 3A, B). The PH domain β-sandwich is formed by a 4-stranded β-sheet on one side (strands β1–β4) packed against a nearly orthogonal 3-stranded β-sheet (strands β5–β7).

In most PH domains, the loops connecting strands β1–2, β3–β4, and β6–β7 extend from the open end of the β-sandwich to create the phosphoinositide-binding pocket. In the DM-PH structure, the PH domains contact the DM domain via a small, but significant interface that primarily involves the β1–β2 loop of each PH domain and a hydrophobic cleft on either side of the DM domain (Figures 1C, 2A). The β1–β2 loop adopts a helical conformation (forming the novel α3 helix) and inserts a hydrophobic residue (Phe132) into a cleft on the DM domain. Four salt bridges, Glu15/Arg195, Asp23/Lys128, Arg18/Asp129 and Asp30/Lys179, contribute to the DM/PH domain interface (Figure 2A, Supplementary Figure 2). Asp129 plays a particularly important structural role by forming an additional salt bridge to Arg127 within the β1–β2 loop that may stabilize its helical conformation (Supplementary Figure 2). The β1–β2 loop is immediately adjacent to the predicted phosphoinositide binding site in the PH domain, and the helical conformation that this loop adopts appears to partially block the phosphoinositide-binding pocket (see below). The linker region between the DM and PH domains (residues 65–109) is disordered. Although the length of the linker precludes unambiguous assignment of connectivity, the shortest path would connect the domains to form the surface contacts described above. The dimer is non-crystallographic, but it is approximately 2-fold symmetric and the two subunits superimpose with an r.m.s. deviation of 0.9 Å.

The Skap-hom dimerization domain

Helices α1 and α2 of the DM domain form a helical hairpin that, together with its counterpart from the second molecule, generates a dimeric, 4-helix bundle (Figures 1C, 2B). The hairpins

from each subunit pack in a parallel manner with 2-fold symmetry about the vertical axis. Within each subunit, α1 and α2 are anti-parallel and cross at an angle of ~30°. Most of the hydrophobic residues in the DM domain project between the helices or into the center of the bundle to form a single hydrophobic core. Six salt-bridges stabilize the domain (Figure 2B, C); four intramolecular (Glu25/Lys56 and Arg18/Glu62 in each subunit) and two intermolecular (between Asp23 in one subunit and Lys51 in the other). The Skap-hom residues involved in the dimer interface are highly conserved in Skap55 (Figure 1B), suggesting that the latter forms an analogous dimer. Indeed, Skap55 behaves as a dimer in solution (Supplementary Figure 1, Supplementary Table 1).

Although the DM domain has no obvious structural counterpart in eukaryotes, a search of the Protein Data Bank using the Dali structural similarity server revealed remote similarity between the DM domain, the Influenza A virus nuclear export protein Nep/Ns2 (Akarsu et al., 2003) and the *Yersinia* secretion protein YscE (Phan et al., 2005). The domain within Nep/Ns2 (PDB ID 1pd3, Dali Z score=6.1) also forms a helical hairpin that dimerizes in a parallel fashion, and its structure superimposes on the DM domain with an r.m.s. deviation of 2.6 Å (Figure 2D). In contrast, the YscE hairpin (PDB ID 1zw0, Dali Z score = 4.9) is an anti-parallel dimer (data not shown). Because the Skap-hom DM domain has no sequence similarity with these other proteins, these structural similarities in domain structure probably arose independently during evolution.

Structural analysis of the Skap-hom PH domain

The helical conformation of the β1–β2 loop in the DM-PH structure is not found in other PH domains and seems incompatible with phosphoinositide binding. We asked whether this conformation might be induced by interaction with the DM domain and represent an inhibited state by determining the crystal structure of the isolated PH domain of Skap-hom to a resolution of 2.1 Å (Table 1) with a crystallographic R factor of 21.3% (R_{free}=27.1%). Consistent with our hypothesis, the β1–β2 loop adopts an open loop conformation in the isolated Skap-hom PH domain (Figures 3A, B). Apart from the dramatic rearrangement of the β1–β2 loop, the structure of the isolated PH domain is essentially the same as that in the DM-PH structure.

Although Skap-hom PH domain binds to 3′ phosphoinositides (see below), we were unable to obtain co-crystals with phosphoinositide head groups. To gain further insight into the likely mode of interaction with phosphoinositides, we compared the Skap-hom PH domain structure to that of the Akt PH domain bound to Ins[1,3,4,5]P_4 (the soluble headgroup of PI[3,4,5]P_3). We chose the latter for comparison because, like the Skap-hom PH domain (see below), it recognizes PI[3,4,5]P_3 and PI[3,4]P_2 (Frech et al., 1997). Akt and Skap-hom also lack the insertions found in the Btk (Baraldi et al., 1999) and Grp1 (Lietzke et al., 2000) PH domains that confer high affinity and specificity for PI[3,4,5]P_3 over PI[3,4]P_2. As shown in Figure 3C, residues Lys125 and Arg140 of Skap-hom superimpose well with Akt residues Lys14 and Arg25, which are key 3′-phosphate binding residues. Like Arg23 in Akt, Gln138 in Skap-hom can hydrogen bond with the 3′-phosphate. The Skap-hom domain also has residues well-positioned to bind the 4′ and 5′-phosphates of the superimposed inositol headgroup, with Tyr151 and Tyr197 approaching the 4′-phosphate position, and the guanidinium group of Arg195 potentially interacting simultaneously with the 4′- and 5′-phosphates (as does Arg86 in Akt, Figure 3C).

This putative phosphoinositide binding pocket is perturbed in the DM-PH structure. The solvent accessible surface of the DM-PH structure, colored coded by electrostatic potential, is shown in Figure 3D (top panel), with the position of the Ins[1,3,4,5]P_4 headgroup modeled on the basis of the Akt superposition in Figure 3C. Formation of the α-helix in the β1–β2 loop partially occludes the phosphoinositol binding pocket, and thus would be expected to preclude binding of phosphoinositides (Figure 3D, lower panels).

The DM domain mediates self-association of Skap-hom *in vivo*

To ask if it can form higher order structures *in vivo*, we co-expressed Flag and HA epitope-tagged versions of Skap-hom in 293T cells. As expected, Flag-Skap-hom co-immunoprecipitated with HA-Skap-hom (Figure 4A). Skap proteins potentially can self-associate via interaction of their C-terminal SH3 domain with a proline-rich segment between the PH and SH3 domains (Wu et al., 2002b). To ascertain whether Skap-hom homodimerization was, in fact mediated by the DM domain, we tested a truncation mutant lacking the SH3 and linker 2 regions (DM-PH), corresponding to the fragment used in our structural analysis. Wild-type DM-PH co-immunoprecipitated with HA-tagged full-length Skap-hom (Figure 4B), showing that the SH3 domain is dispensable for dimerization *in vivo*. On the other hand, a Skap-hom DM-PH construct bearing three point mutations in the dimerization interface (V24D, F27D and V28E, termed DM*-PH) failed to dimerize with the WT protein (Figure 4B). A full-length Skap-hom mutant bearing the same mutations also failed to dimerize (Supplementary Figure 3A). Because the DM domain appears to require dimerization for proper folding, we expect that the DM* mutant is locally unfolded or misfolded. The DM* mutant is not, however, globally disrupted, because the full length DM* mutant is still binds Adap (presumably via its C-terminal SH3 domain, Supplementary Figure 3B). Thus, consistent with our crystal structure, the N-terminal dimerization domain is required for self-association of Skap-hom *in vivo*.

The Skap-hom PH Domain Binds PI[3,4]P_2 and PI[3,4,5]P_3

We next evaluated the lipid binding properties of the Skap-hom PH domain. Using phospholipids immobilized in a “dot-blot” format, we found that the Skap-hom PH domain binds to PI[3,4]P_2 or PI[3,4,5]P_3, the products of phosphatidylinositol 3-kinase (PI3K), but not to PI[3]P, PI[5]P or PI[4,5]P_2 (Figure 5A, left panel). Consistent with the contortion of the PH domain noted in the crystal structure (Figure 3D), binding of the DM-PH fragment to PI[3,4]P_2 and PI[3,4,5]P_3 was weaker (Figure 5A, right panel). To quantify binding more precisely, we employed a florescence polarization-based assay (Figures 5B, C) that uses soluble, short-chain phospholipids bearing a fluorescent label and permits measurement of equilibrium binding in solution (Ceccarelli et al., 2007). The PH domain of Skap-hom bound with highest affinity to PI[3,4,5]P_3 (K_d =8 μM), but also showed significant PI[3,4]P_2 binding (K_d=40 μM; Figure 5B and data not shown). Binding of Skap-hom to PI(4,5)P_2 and PI(3,5)P_2 was too weak to quantify using this assay (data not shown). Consistent with the dot-blot assays, the presence of the DM domain reduced the affinity of Skap-hom for PI[3,4,5]P_3 to ~30 μM and for PI[3,4]P_2 to 90 μM (Figure 5C and data not shown). Like the Akt PH domain mutated at the corresponding residue R25 (Thomas et al., 2003), Skap-hom bearing an R140M mutation in the putative phosphoinositide binding pocket is defective in PI[3,4,5]P_3 binding (Kd >100 μM; Figure 5B).

To further probe the potential relevance of the interface in the regulation of PI[3,4,5]P_3 binding, we generated mutations predicted to perturb docking between the PH and DM domains (E15R, F132A, K56A, D129A, and D129K; Figure 5C and data not shown). The K56A mutant had lipid-binding affinity similar to WT (Kd = 30 μM), but the D129K mutant showed much higher affinity (6 μM), comparable to that of the isolated PH domain. The more conservative D129A mutant had an intermediate affinity (20 μM).

Skap-hom is controlled by a DM/PH domain switch

To better understand the significance of dimerization and the DM/PH interface in Skap-hom function, we carried out structure-function studies in Skap-hom$^{-/-}$ bone marrow-derived macrophages (BMM; Figure 6, Supplementary Figure 6 and Supplementary Movies). In WT BMM, Skap-hom localizes to actin-rich membrane ruffles. In Skap-hom$^{-/-}$ BMM, ruffling is initiated, but ruffle formation is impaired (Supplemental Movies and KDS and BGN,

manuscript in preparation). Retrovirus-mediated expression of WT Skap-hom-GFP restored ruffling, and the GFP-tagged protein concentrated in actin-rich membrane ruffles (Figures 6A, H and O). Immunostaining with Skap-hom-specific antibodies revealed similar localization of the Skap-hom-GFP and endogenous Skap-hom (Supplementary Figure 4). In contrast, GFP alone was distributed diffusely, with only a minor fraction randomly co-localized with cytoskeletal structures (Figures 6B, I, and P). A dimerization domain mutant (DM*, the triple-mutant described above) and the PH domain mutant unable to bind phosphoinositides (R140M) showed defective association with ruffles (Figure 6, panels C, J, Q and D, K, R, respectively). Thus, proper sub-cellular localization of Skap-hom requires a functional DM domain and the ability to bind 3′-phosphinositides. Cells expressing these mutant Skap-hom proteins also had less robust ruffles, consistent with a role for Skap-hom in ruffle generation (Figure 6, panels J and K vs. panel H).

In a simple model, the PH domain would function to target Skap-hom to regions of the membrane expressing 3′ phosphoinositides. However, in contrast to the R140M mutant, a PH domain deletion mutant (ΔPH Skap-hom; see Figure 1A) retained association with actin-rich ruffles, exhibiting a pattern indistinguishable from that of WT Skap-hom (Figures 6E, L and S). These findings pose an apparent paradox: why does a mutant lacking the entire PH domain retain targeting, whereas the R140M point mutant does not? Conceivably, the PH domain plays no role in Skap-hom localization, in which case our results could be explained by neomorphic effects of the R140M mutation (e.g., local misfolding leading to aggregation or mislocalization of Skap-hom R140M). But treatment of BMM expressing WT Skap-hom-GFP with the PI3K inhibitor Ly294002 also resulted in dissociation of Skap-hom from the actin cytoskeleton, indicating that PH domain binding to 3′ phosphoinositides is, in fact, required for normal targeting of the WT protein (Supplementary Figure 5). These results, and our structural and lipid binding data, which indicate mutually exclusive binding of the PH domain to the DM domain and 3′ phosphoinositides, respectively, suggested an alternative model in which the (unliganded) PH domain inhibits Skap-hom ruffle association, and auto-inhibition is reversed by 3′ phosphoinositides. In this model, the deletion mutant would be constitutively active, whereas the R140M point mutant would be locked in the auto-inhibited state.

To test this model, we examined the localization of GFP-Skap-hom fusion proteins bearing the mutations D129K, D129A, K56A, E15R, or F132A, which are expected to perturb the interface between the DM and PH domains. None of these mutations interfered with recruitment to ruffles (Supplementary movies and data not shown), indicating that DM/PH domain interaction is not required for ruffle association. We also tested double mutants that combine the D129K and K56A mutations in the interface with the R140M mutation in the phosphoinositide binding pocket (D129K:R140M and K56A:R140M). These mutations should simultaneously block phosphoinositide binding and perturb the interaction between the DM and PH domains. Strikingly, the double mutants localized to ruffles to an extent similar to that of WT Skap-hom (Figure 6, compare panels F, M, T and G, N, U with WT panels A, H, O; see also Supplementary Movies). Thus, disruption of the DM/PH domain interface dominates over defective phosphoinositide binding in promoting Skap-hom localization to ruffles, and supports a model in which phosphoinositide binding to the PH domain controls its ability to interact with the DM domain (Supplementary Figure 7). These data also argue against neomorphic effects of the R140M mutation, because this mutation does not cause mislocalization when the D129K or K56A mutations are superimposed.

As a further test of the effects of these mutants on localization of Skap-hom, we performed fluorescent time-lapse photomicroscopy of Skap-hom$^{-/-}$ BMM reconstituted with WT Skap-hom or the above mutants (see Supplementary Figure 6 and Supplementary Movies). Whereas WT Skap-hom-GFP localized in sharply defined, dynamic wave-like structures that co-localize with co-expressed mCherry-tagged actin (Supplementary Movie J), the R140M and DM

mutants were more diffusely distributed and lacked discrete ruffle association, similar to the GFP control (Supplementary Movies D and A). Most importantly, Skap-hom$^{-/-}$ BMM expressing the ΔPH domain, D129K, D129K:R140M, K56A or K56A:R140M mutants all exhibited similar, wave-like accumulations of the GFP-tagged protein essentially indistinguishable from those seen in cells reconstituted with WT Skap-hom (see Supplementary Movies E through I).

Discussion

PH domains frequently target adaptors and other signaling components to specific membranous regions in cells (Lemmon, 2003). Here, we have found that the Skap-hom PH domain regulates intracellular targeting in a different way: in concert with the DM domain, it acts as 3′ phosphoinositide-gated switch to control exposure of a distinct targeting domain and, consequently, association of Skap-hom with actin-based ruffles in macrophages. Our proposed model is supported by structural, biochemical and biological evidence and has implications for the function of Skap-hom.

Skap-hom dimerizes via the N-terminal DM domain

Using structure prediction algorithms, previous workers concluded that Skap-hom, but not Skap55, contained a coiled-coil domain that might mediate dimerization (Marie-Cardine et al., 1998). Other studies suggested that Skap55 self-associates via its SH3 domain and proline-rich stretch (Wu et al., 2002). Our biochemical and structural studies show that Skap-hom contains a dimerization domain in its N-terminus, but rather than adopting a simple coiled-coiled structure as predicted, the DM domain comprises a four-helix bundle formed by the intimate association of “helical hairpin” elements from each of the two monomers. The corresponding region in Skap55 most likely forms a similar dimer, as nearly all of the residues in the dimer interface are conserved in Skap55 (Figure 1B). Indeed, Skap55 also forms dimers *in vitro* (Supplementary Figure 1). We have not explicitly tested whether Skap proteins self-associate via their SH3 domains (Wu et al., 2002). However, Skap-hom clearly dimerizes in the absence of its SH3 domain, and the DM domain is necessary for dimerization (Figure 4 and Supplementary Figure 3A). Most likely, the same is also true for Skap55.

The Skap-hom DM and PH domains comprise a phosphoinositide-gated switch

The isolated Skap-hom PH domain binds preferentially to PI[3,4,5]P_3 (Figure 5). When the DM domain is present, though, the β1–β2 loop of the PH domain forms a short helix that packs into a hydrophobic groove on the DM domain. The DM/PH domain interaction probably precludes binding of 3′ phosphoinositides to the PH domain for at least two reasons. First, the helix formed by the β1–β2 loop sterically blocks a portion of the predicted phosphoinositide binding pocket (Figure 3D). Moreover, basic residues that are expected to hydrogen bond with the phospholipid head group make alternative interactions in the “docked” DM-PH structure (Figure 2A).

Consistent with our structural data, the affinity of the DM-PH construct for 3′ phosphoinositides is decreased relative to that of the free PH domain (Figure 5C), whereas mutations predicted to disrupt the interface promote higher affinity binding. In particular, the D129K charge reversal mutation confers affinity equivalent to that of the isolated PH domain. It is not clear why the K56A mutation does not show increased affinity; conceivably, it does not sufficiently shift the equilibrium to the undocked state under our assay conditions.

The potential for allosteric inhibitory interactions between its DM and PH domains suggests that Skap-hom exists in two-states with distinct 3′ phosphoinositide-binding abilities: a closed, inactive, “docked” state, and an open, “free” conformation capable of lipid binding (Figure 7).

The DM-PH crystal structure represents the docked, auto-inhibited conformation, whereas the isolated PH domain structure presumably represents the free state. We expect that the residual phosphoinositide binding observed *in vitro* with the DM-PH protein stems from an equilibrium between the docked and free states. We further propose that in the cellular context, transition between these states is governed by binding of the PH domain to 3′ phosphoinositides, and thus by PI-3 kinases and phosphatases. The high degree of conservation of the residues comprising this switch suggests that Skap55 is likely to be regulated similarly.

This "gated-switch" mechanism has important consequences. First, the dimeric structure of the free conformation provides a large boost in apparent affinity (due to avidity effects) to the relatively weak monomer binding to PI[3,4,5]P_3-rich membranes. Surprisingly, however, the ΔPH Skap-hom protein still localizes efficiently to ruffles; consequently, 3′ phosphoinositide binding cannot be the primary determinant of Skap-hom localization. Instead, the second major implication of our results is that phosphoinositide-induced undocking of the PH domains unmasks a distinct ruffle-targeting signal. Furthermore, the increase in effective lipid binding ability expected for the "two-headed" Skap-hom PH domain structure may confer ultrasensitivity to the targeting process.

The precise nature/location of the ruffle-targeting signal in Skap-hom remains to be delineated. In the simplest model, it would reside within Skap-hom itself. If so, mutagenesis experiments indicate that it must lie outside of the PH domain (Figure 6 and data not shown). A particularly attractive possibility is that it is located on the surface of the DM domain, overlapping with the docking site of the PH domain. Indeed, disrupting the DM domain (i.e., in the mutant DM*) abolishes proper sub-cellular targeting. However, the DM* mutant also cannot dimerize, so dimerization, rather than a specific motif within the DM domain, could be required indirectly for localization (e.g., to create or expose a targeting motif elsewhere in Skap-hom). Distinguishing between these possibilities will require finer mutagenesis of the DM domain to see if targeting and dimerization can be separated. Notably, the D129K and K56A mutations in the DM domain do target appropriately. Alternatively, we cannot exclude the possibility that the targeting motif masked by the Skap-hom PH domain residues in a Skap-hom-associated protein. In this regard, only the Skap55/Adap complex (and not either monomer) can bind Riam1 (Kliche et al., 2006).

The Skap-hom PH and DM domains engage in a process of mutual allosteric inhibition, a strategy encountered repeatedly, though in different guises, in signal transduction. For example, the N-SH2 domain of the protein-tyrosine phosphatase Shp2 interacts with the catalytic (PTP) domain, rendering the enzyme inactive until phosphotyrosyl peptides that bind the N-SH2 domain are encountered. There too, the structure of the phosphotyrosyl peptide-bound SH2 domain is incompatible with SH2/PTP domain interaction (Hof et al., 1998). Likewise, the RAC binding site and one of the two RAS binding sites in the guanine nucleotide exchange factor SOS1 is blocked by a lipid-gated PH/DH module (Soisson et al., 1998; Sondermann et al., 2004), whereas exposure of the VCA domains of Wasp family proteins can be regulated by the binding of small G proteins, adaptors such as Nck, or phospholipids (Takenawa and Miki, 2001).

Biological implications

Skap-hom$^{-/-}$ macrophages exhibit reduced ruffling, and mutants that fail to target correctly also fail to restore normal ruffling (Figure 6 and Supplementary Movies). Ruffle formation is also decreased dramatically in BMM treated with PI 3-kinase inhibitors (Wheeler et al., 2006 and Supplementary Figure 5). Consequently, it is difficult to be certain whether "gating" by PI[3,4,5]P_3 controls targeting *per se*, ruffle generation, or both.

We suspect that proper targeting is required to promote ruffle generation, which may then lead to additional recruitment of Skap-hom. Ruffling probably requires 3′ phosphoinositides at multiple stages. Rac-GEFs, such as Vav and αPix, comprise one class of 3′ phosphoinositide-binding proteins critical for actin polymerization (Han et al., 1998; Yoshii et al., 1999). *A priori*, there is no reason to suspect a role for Skap-hom in Rac-GEF activation; consequently, initiation of ruffling should be unaffected by Skap-hom deficiency. Indeed, small ruffles do appear in Skap-hom$^{-/-}$ BMM, but ruffling is not sustained (Supplementary Movies). Abortive ruffling may well be the consequence of the lack of Skap-hom and its partner protein Adap in the nascent ruffle. Adap associates with Vasp (Krause et al., 2000) and the Arp2/3 activating protein, Wasp (Coppolino et al., 2001), partners that could enhance and sustain actin polymerization, and thereby yield robust ruffling. Alternatively, as like Skap55 (Kliche et al., 2006; Menasche et al., 2007), Skap-hom/Adap complexes may bind Riam1 and promote further integrin activation and actin reorganization.

Regardless of the precise mechanistic details, our key finding is that the novel structure of the DM-PH module controls these processes. Furthermore, the switch-like regulation of Skap-hom by 3′ phosphoinositides conforms perfectly to its role mediating dynamic cytoskeletal rearrangements.

Experimental Procedures

Cloning, Protein Expression and Purification

Murine Skap-hom cDNA (Swiss-Prot accession number Q9Z2K4) was amplified by RT-PCR and cloned into the pEGFP N1 (Clonetech). This fusion gene was subcloned into pMXPuro (Kitamura et al., 2003), creating pMXSskaphom WT. Skap-hom-flag was created by PCR and cloned into a C-terminal p3Xflag-CMV vector (Sigma-Aldrich). Full-length Skap-hom ΔPH construct was created by standard mutagenesis to remove nucleotides encoding residues (118–222). Point mutants were generated by PCR-based overlapping mutagenesis; primer sequences are available from K.D.S. upon request. The 6X His-tagged DM-PH construct was generated by PCR and cloned into pCDNA6XHis (Invitrogen).

To prepare Skap-hom proteins, DNA fragments encoding residues 101–222 (PH domain) or 14–222 (DM-PH) of mouse Skap-hom were cloned into a modified pET vector (Novagen) to generate GST-fusions. Recombinant proteins were expressed in *E. coli* BL21(DE3) cells at 18 °C, followed by lysis in PBS-βME (5mM β-mercaptoethanol) containing lysozyme and Complete® protease inhibitor (Roche, Germany). Lysates were cleared by centrifugation at 18K RPM for 45 minutes at 4 °C, and supernatants were incubated with glutathione beads pre-equilibrated with PBS-βME. The beads were then washed extensively with PBS-βME before final equilibration with elution buffer (EB) (25 mM PIPES, 150 mM NaCl, 5 mM DTT, pH6.5). GST-fusion proteins were cleaved from the beads by incubating with TEV protease overnight at 20°C. The resultant Skap-hom proteins contain two vector amino acids, Gly-Ser, at their N-termini, and were purified by ion-exchange chromatography, using a sodium chloride gradient from 50 to 1000 mM in EB. Protein fractions were pooled and concentrated for a final purification on a Superdex 75 column. Final eluates were concentrated, and stored in aliquots at −70 °C.

Crystallization and structure determination

Crystallization experiments were carried out by hanging-drop vapor diffusion at 20 °C. The Skap-hom PH domain (7.5 mg/ml in EB) crystallized over a reservoir solution of 20% (w/v) PEG 4000, 100 mM Tris-HCl pH7.6, and 150 mM NaCl; the Skap-hom DM-PH protein (12 mg/ml in EB) crystallized over a reservoir solution of 24% (w/v) PEG 4000 and 100mM Hepes pH7.6. Protein crystals were briefly transferred to cryo-protectant solutions before freezing

with liquid nitrogen. X-ray diffraction data were collected under nitrogen gas at 100 K using either a Mar image plate system (MAR Research, Hamburg, Germany, for Skap-hom PH) or the synchrotron source at CHESS A1 (for Skap-hom DM-PH). Reflection intensities were integrated and scaled by DENZO and SCALEPACK, respectively, (Otwinowski and Minor, 1997) (see Table 1).

The Skap-hom PH and DM-PH structures were determined by molecular replacement using the program COMO (Jogl et al., 2001). An alternate crystal form of the Skap-hom PH domain (PDB ID 1U5F) was used as a search model; this alternate structure was determined by heavy-atom methods (See Supplementary Methods). The model for the DM domain of Skap-hom DM-PH was built manually using difference Fourier maps calculated with initial phases derived from the molecular replacement solution for the two PH domains in the asymmetric unit. The DM-PH and PH domain structures were improved further by iterative manual refitting with the program O (Jones et al., 1991) and crystallographic refinement with the program CNS (Brunger et al., 1998); see Table 1. Model quality and accuracy were assessed by PROCHECK (Laskowski et al., 1993). No density was observed for residues 101–104 and 220–222 in the Skap-hom PH domain or residues 65–105 in the Skap-hom DM-PH structure.

Lipid Dot Blots and Fluorescence Polarization Assays

For dot blot assays, the indicated phosphoinositides were dissolved in methanol:chloroform:water and spotted onto Hybond-C Extra membranes (Amersham) at the indicated concentrations. Lipid-containing membranes were incubated in TBS (10 mM Tris-HCl pH 7.4, 150 mM NaCl) containing fat-free bovine serum albumin (BSA), 0.5 mM EDTA, and the indicated proteins. Bound proteins were detected using rabbit polyclonal antibodies directed against GST (Rockland, Gilbertsville, PA) and IR 800-labeled goat anti-rabbit secondary antibodies. Secondary antibodies were detected using an Odyssey reader (Li-Cor, Lincoln, NE). The affinities of binding of PI[3,4]P_2 and PI[3,4,5]P_3 to Skap-hom PH and DM-PH proteins were determined by fluorescence polarization (FP) using BODIPY TMR-X-labeled short chain and soluble phosphatidylinositol phosphates (Ceccarelli et al., 2007). Briefly, increasing amounts of purified protein were added to 12.5 nM fluorescent phospholipid in EB. After incubation at room temperature for 20 minutes, the FP signal was measured in triplicate at 21 °C using a Beacon 2000 FP system. Polarization filters were selected to match the excitation and emission spectra (542 nm and 574 nm, respectively) for the TMR-X fluorescent label. Binding curves and constants were generated using GraphPad Prism (GraphPad Software Inc.).

Mice, cell culture and retroviral gene transduction

Skap-hom$^{-/-}$ mice (Balb/c) were (Togni et al., 2005), were maintained under pathogen-free conditions and used at 8–12 weeks. All studies were approved by the Institutional Animal Care Committee of Beth Israel Deaconess Medical Center.

BMM were differentiated *ex vivo* as described (Tushinski et al., 1982), and analyzed after 7 days in culture. HEK293 T/17 cells (Pear et al., 1993) were maintained in 10% FCS and 10% CO_2 at 37°C. Retroviruses were produced by co-transfecting pEcoPAK (Clonetech) and pMXPuro constructs bearing the inserts indicated in the figure legends into in HEK293T/17 cells, using polyethylenimine (Polysciences Inc) (Godbey et al., 2000). Viruses were harvested 48 hours post-infection and used to infect bone marrow cultures.

Immunoprecipitation and immunoblotting

For whole cell extracts, cells were washed in phosphate buffered saline (PBS), and lysed (on plates) in Nonidet P-40 (NP-40) lysis buffer (1% NP-40, 50 mM Tris-HCl pH 7.4, 150 mM NaCl, 100 μM pervanadate, protease inhibitors). Lysates were clarified in a microcentrifuge

at 4°C for 10 min and protein concentrations were determined using a bicinchoninic acid protein assay reagent kit (Pierce). Immune precipitations were performed by adding antibodies plus protein A-Sepharose beads to lysates and incubating at 4°C for 2 hrs. Immune complexes were washed with lysis buffer, resolved by SDS-PAGE, and transferred onto Immobilon-FL membranes (Millipore). Immunoblots were blocked with 5% BSA in TBS with 0.05% Tween 20 (TBST) for 1 hr, incubated for 1 hr with primary antibodies in TBST, washed three times for 10 min each in TBST, and then incubated for 1 hr with IR 680-labeled anti-mouse IgG (Invitrogene) or IR 800-labeled anti-rabbit IgG (Rockland, Gilbertsville, PA) which were detected as described above.

Microscopy

Skap-hom$^{-/-}$ BMM expressing GFP-tagged Skap-hom proteins were fixed in 4% PFA, 25 mM PIPES pH 6.8, 129 mM KCl, 20 % sucrose, 5mM EDTA and permeabilized in 0.05% Triton X-100 in PBS, pH 7.4. For immunofluorescence, cells were stained with rhodamine phalloidin (Invitrogen) and rabbit anti-Skap-hom (Upstate-Millipore) in 1X PBS containing 3% BSA. Bound antibodies were visualized using Alexa488-conjugated anti-rabbit IgG (Invitrogen) and observed under oil immersion using a Zeiss Axiovert 200M microscope with a 63X Plan-Apochromat objective with a numerical aperture of 1.4. Images were analyzed using the iterative deconvolution program within the Axiovision 4.5 software package.

Accession numbers

Atomic coordinates and structure factors for the two structures reported here have been deposited with the Protein Data Bank (http://www.rcsb.org/) with accession codes 1U5G (Skap-hom PH) and 2OTX (Skap-hom DM-PH).

Supplementary Material

Refer to Web version on PubMed Central for supplementary material.

Acknowledgements

We thank Q. Hao at MacCHESS beamline A1, T. Boggon and Y. Xu for assistance with data collection, R. Marmorstein for critical reading of the manuscript, F. Sicheri for help with fluorescence polarization, and L.C. Cantley for his support. This work was supported by NIH grants R01CA080942 and P01HL048675 to M.J.E., grants R37CA 41952 and R01CA114945 to B.G.N and 2T32 HL07623-23 to K.D.S and the Canadian Institute of Health Research, the Canadian-Strategic Training in Health Research fellowship to D.F.C. pEBHA-Fyb and mCherry tagged-actin were gifts from Chris Rudd (University of Cambridge) and Max Krummel (UCSF), respectively.

References

Akarsu H, Burmeister WP, Petosa C, Petit I, Müller CW, Ruigrok RW, Baudin F. Crystal structure of the M1 protein-binding domain of the influenza A virus nuclear export protein (NEP/NS2). EMBO J 2003;22:4646–4655. [PubMed: 12970177]

Baraldi E, Djinovic Carugo K, Hyvonen M, Surdo PL, Riley AM, Potter BV, O'Brien R, Ladbury JE, Saraste M. Structure of the PH domain from Bruton's tyrosine kinase in complex with inositol 1,3,4,5-tetrakisphosphate. Structure 1999;7:449–460. [PubMed: 10196129]

Black DS, Marie-Cardine A, Schraven B, Bliska JB. The Yersinia tyrosine phosphatase YopH targets a novel adhesion-regulated signalling complex in macrophages. Cell Microbiol 2000;2:401–414. [PubMed: 11207596]

Bourette RP, Therier J, Mouchiroud G. Macrophage colony-stimulating factor receptor induces tyrosine phosphorylation of Skap55R adaptor and its association with actin. Cell Signal 2005;17:941–949. [PubMed: 15894167]

Brunger AT, Adams PD, Clore GM, DeLano WL, Gros P, Grosse-Kunstleve RW, Jiang JS, Kuszewski J, Nilges M, Pannu NS, et al. Crystallography & NMR system: A new software suite for

macromolecular structure determination. Acta Crystallogr D Biol Crystallogr 1998;54:905–921. [PubMed: 9757107]

Ceccarelli DF, Blasutig IM, Goudreault M, Li Z, Ruston J, Pawson T, Sicheri F. Non-canonical interaction of phosphoinositides with pleckstrin homology domains of Tiam1 and ArhGAP9. J Biol Chem 2007;282:13864–13874. [PubMed: 17339315]

Coppolino MG, Krause M, Hagendorff P, Monner DA, Trimble W, Grinstein S, Wehland J, Sechi AS. Evidence for a molecular complex consisting of Fyb/SLAP, SLP-76, Nck, Vasp and WASP that links the actin cytoskeleton to Fcgamma receptor signalling during phagocytosis. J Cell Sci 2001;114:4307–4318. [PubMed: 11739662]

Curtis DJ, Jane SM, Hilton DJ, Dougherty L, Bodine DM, Begley CG. Adaptor protein Skap55R is associated with myeloid differentiation and growth arrest. Exp Hematol 2000;28:1250–1259. [PubMed: 11063873]

da Silva AJ, Li Z, de Vera C, Canto E, Findell P, Rudd CE. Cloning of a novel T-cell protein FYB that binds FYN and SH2-domain-containing leukocyte protein 76 and modulates interleukin 2 production. Proc Natl Acad Sci U S A 1997;94:7493–7498. [PubMed: 9207119]

Fallman M, Deleuil F, McGee K. Resistance to phagocytosis by Yersinia. Int J Med Microbiol 2002;291:501–509. [PubMed: 11890550]

Godbey WT, Barry MA, Saggau P, Wu KK, Mikos AG. Poly(ethylenimine)-mediated transfection: a new paradigm for gene delivery. J Biomed Mater Res 2000;51:321–328. [PubMed: 10880073]

Frech M, Andjelkovic M, Ingley E, Reddy KK, Falck JR, Hemmings BA. High affinity binding of inositol phosphates and phosphoinositides to the pleckstrin homology domain of RAC/protein kinase B and their influence on kinase activity. J Biol Chem 1997;272:8474–8481. [PubMed: 9079675]

Griffiths EK, Krawczyk C, Kong YY, Raab M, Hyduk SJ, Bouchard D, Chan VS, Kozieradzki I, Oliveira-Dos-Santos AJ, Wakeham A, et al. Positive regulation of T cell activation and integrin adhesion by the adapter Fyb/Slap. Science 2001;293:2260–2263. [PubMed: 11567140]

Han J, Luby-Phelps K, Das B, Shu X, Xia Y, Mosteller RD, Krishna UM, Falck JR, White MA, Broek D. Role of substrates and products of PI 3-kinase in regulating activation of Rac-related guanosine triphosphatases by Vav. Science 1998;279:558–560. [PubMed: 9438848]

Hof P, Pluskey S, Dhe-Paganon S, Eck MJ, Shoelson SE. Crystal structure of the tyrosine phosphatase SHP-2. Cell 1998;92:441–450. [PubMed: 9491886]

Huang Y, Norton DD, Precht P, Martindale JL, Burkhardt JK, Wange RL. Deficiency of ADAP/Fyb/SLAP-130 destabilizes Skap55 in Jurkat T cells. J Biol Chem 2005;280:23576–23583. [PubMed: 15849195]

Jogl G, Tao X, Xu Y, Tong L. COMO: a program for combined molecular replacement. Acta Crystallogr D Biol Crystallogr 2001;57:1127–1134. [PubMed: 11468396]

Jones TA, Zou JY, Cowan SW, Kjeldgaard M. Improved methods for building protein models in electron density maps and the location of errors in these models. Acta Cryst 1991;A47:110–119.

Kitamura T, Koshino Y, Shibata F, Oki T, Nakajima H, Nosaka T, Kumagai H. Retrovirus-mediated gene transfer and expression cloning: powerful tools in functional genomics. Exp Hematol 2003;31:1007–1014. [PubMed: 14585362]

Kliche S, Breitling D, Togni M, Pusch R, Heuer K, Wang X, Freund C, Kasirer-Friede A, Menasche G, Koretzky GA, Schraven B. The ADAP/Skap55 signaling module regulates T-cell receptor-mediated integrin activation through plasma membrane targeting of Rap1. Mol Cell Biol 2006;26:7130–7144. [PubMed: 16980616]

Kouroku Y, Soyama A, Fujita E, Urase K, Tsukahara T, Momoi T. RA70 is a src kinase-associated protein expressed ubiquitously. Biochem Biophys Res Commun 1998;252:738–742. [PubMed: 9837776]

Krause M, Sechi AS, Konradt M, Monner D, Gertler FB, Wehland J. Fyn-binding protein (Fyb)/SLP-76-associated protein (SLAP), Ena/vasodilator-stimulated phosphoprotein (Vasp) proteins and the Arp2/3 complex link T cell receptor (TCR) signaling to the actin cytoskeleton. J Cell Biol 2000;149:181–194. [PubMed: 10747096]

Laskowski RA, MacArthur MW, Moss DS, Thornton JM. PROCHECK: a program to check the stereochemical quality of protein structures. J Appl Cryst 1993;26:283–291.

Lemmon MA. Phosphoinositide recognition domains. Traffic 2003;4:201–213. [PubMed: 12694559]

Lemmon MA. Pleckstrin homology domains: not just for phosphoinositides. Biochem Soc Trans 2004;32:707–711. [PubMed: 15493994]

Lietzke SE, Bose S, Cronin T, Klarlund J, Chawla A, Czech MP, Lambright DG. Structural basis of 3-phosphoinositide recognition by pleckstrin homology domains. Mol Cell 2000;6:385–394. [PubMed: 10983985]

Marie-Cardine A, Bruyns E, Eckerskorn C, Kirchgessner H, Meuer SC, Schraven B. Molecular cloning of Skap55, a novel protein that associates with the protein tyrosine kinase p59fyn in human T-lymphocytes. J Biol Chem 1997;272:16077–16080. [PubMed: 9195899]

Marie-Cardine A, Verhagen AM, Eckerskorn C, Schraven B. SKAP-HOM, a novel adaptor protein homologous to the FYN-associated protein Skap55. FEBS Lett 1998;435:55–60. [PubMed: 9755858]

Menasche G, Kliche S, Chen EJ, Stradal TE, Schraven B, Koretzky G. RIAM links the ADAP/SKAP-55 signaling module to Rap1, facilitating T-cell-receptor-mediated integrin activation. Mol Cell Biol 2007;27:4070–4081. [PubMed: 17403904]

Pear WS, Nolan GP, Scott ML, Baltimore D. Production of high-titer helper-free retroviruses by transient transfection. Proc Natl Acad Sci U S A 1993;90:8392–8396. [PubMed: 7690960]

Peterson EJ, Woods ML, Dmowski SA, Derimanov G, Jordan MS, Wu JN, Myung PS, Liu QH, Pribila JT, Freedman BD, et al. Coupling of the TCR to integrin activation by Slap-130/Fyb. Science 2001;293:2263–2265. [PubMed: 11567141]

Phan J, Austin BP, Waugh DS. Crystal structure of the Yersinia type III secretion protein YscE. Protein Sci 2005;14:2759–2763. [PubMed: 16195558]

Simeoni L, Kliche S, Lindquist J, Schraven B. Adaptors and linkers in T and B cells. Curr Opin Immunol 2004;16:304–313. [PubMed: 15134779]

Soisson SM, Nimnual AS, Uy M, Bar-Sagi D, Kuriyan J. Crystal structure of the Dbl and pleckstrin homology domains from the human Son of Sevenless protein. Cell 1998;95:259–268. [PubMed: 9790532]

Sondermann H, Soisson SM, Boykevisch S, Yang SS, Bar-Sagi D, Kuriyan J. Structural analysis of autoinhibition in the Ras activator Son of Sevenless. Cell 2004;119:393–405. [PubMed: 15507210]

Takenawa T, Miki H. WASP and WAVE family proteins: key molecules for rapid rearrangement of cortical actin filaments and cell movement. J Cell Sci 2001;114:1801–1809. [PubMed: 11329366]

Thomas CC, Deak M, Alessi DR, van Aalten DM. High-resolution structure of the pleckstrin homology domain of protein kinase b/akt bound to phosphatidylinositol (3,4,5)-trisphosphate. Curr Biol 2002;12:1256–1262. [PubMed: 12176338]

Timms JF, Swanson KD, Marie-Cardine A, Raab M, Rudd CE, Schraven B, Neel BG. SHPS-1 is a scaffold for assembling distinct adhesion-regulated multi-protein complexes in macrophages. Curr Biol 1999;9:927–930. [PubMed: 10469599]

Togni M, Swanson KD, Reimann S, Kliche S, Pearce AC, Simeoni L, Reinhold D, Wienands J, Neel BG, Schraven B, Gerber A. Regulation of in vitro and in vivo immune functions by the cytosolic adaptor protein SKAP-HOM. Mol Cell Biol 2005;25:8052–8063. [PubMed: 16135797]

Tushinski RJ, Oliver IT, Guilbert LJ, Tynan PW, Warner JR, Stanley ER. Survival of mononuclear phagocytes depends on a lineage-specific growth factor that the differentiated cells selectively destroy. Cell 1982;28:71–81. [PubMed: 6978185]

Wang H, Liu H, Lu Y, Lovatt M, Wei B, Rudd CE. Functional defects of SKAP-55-deficient T cells identify a regulatory role for the adaptor in LFA-1 adhesion. Mol Cell Biol 2007;27:6863–6875. [PubMed: 17646386]

Wang H, Moon EY, Azouz A, Wu X, Smith A, Schneider H, Hogg N, Rudd CE. SKAP-55 regulates integrin adhesion and formation of T cell-APC conjugates. Nat Immunol 2003;4:366–374. [PubMed: 12652296]

Wegener KL, Partridge AW, Han J, Pickford AR, Liddington RC, Ginsberg MH, Campbell ID. Structural basis of integrin activation by talin. Cell 2007;128:171–182. [PubMed: 17218263]

Wheeler AP, Smith SD, Ridley AJ. CSF-1 and PI 3-kinase regulate podosome distribution and assembly in macrophages. Cell Motil Cytoskeleton 2006;63:132–140. [PubMed: 16421924]

Wu L, Yu Z, Shen SH. Skap55 recruits to lipid rafts and positively mediates the MAPK pathway upon T cell receptor activation. J Biol Chem 2002;277:40420–40427. [PubMed: 12171928]

Yoshii S, Tanaka M, Otsuki Y, Wang DY, Guo RJ, Zhu Y, Takeda R, Hanai H, Kaneko E, Sugimura H. alphaPIX nucleotide exchange factor is activated by interaction with phosphatidylinositol 3-kinase. Oncogene 1999;18:5680–5690. [PubMed: 10523848]

Zhao C, Du G, Skowronek K, Frohman MA, Bar-Sagi D. Phospholipase D2-generated phosphatidic acid couples EGFR stimulation to Ras activation by Sos. Nat Cell Biol 2007;9:706–712. [PubMed: 17486115]

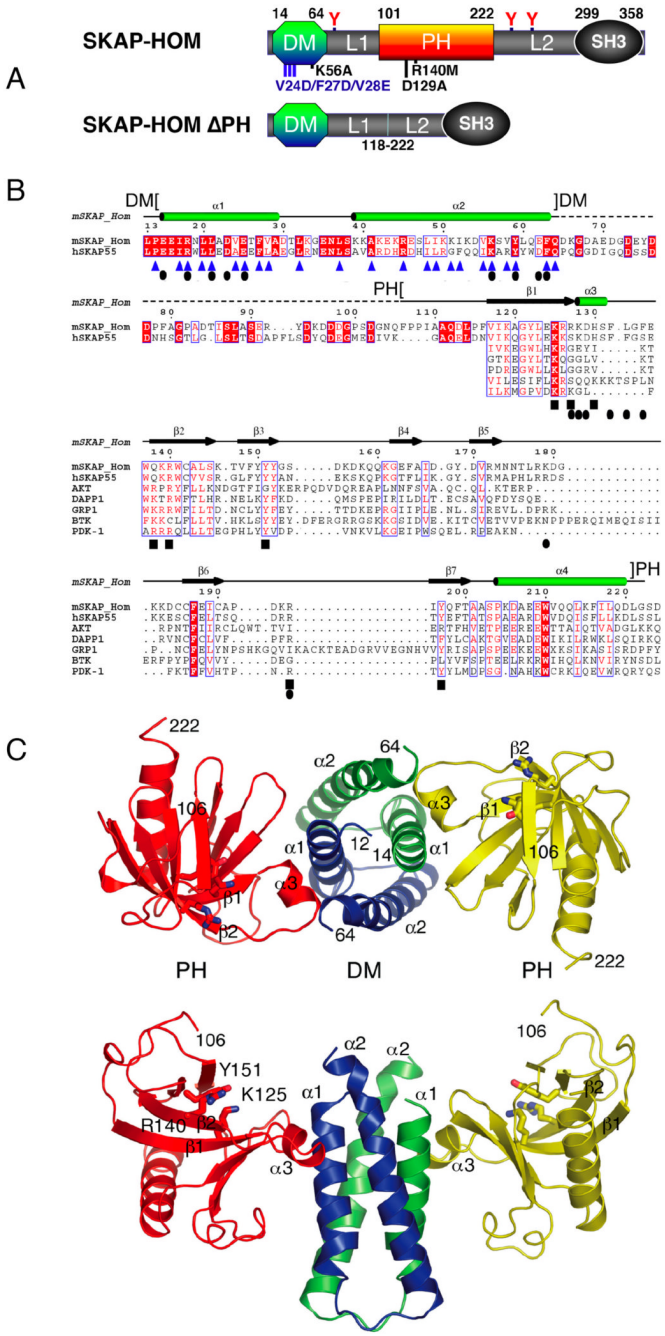

Figure 1.

Structure of Skap-hom. (A) Schematic showing Skap-hom dimerization (DM), PH and SH3 domains, and two intervening linkers (L). Potential tyrosine phosphorylation (Y) sites are indicated, and point mutations studied herein are indicated below. The domain structure of the Skap-hom ΔPH mutant is also shown. (B) Structure-based sequence alignment of the Skap-hom and Skap55 N-termini and selected PH domains. Identical residues are shaded red, highly conserved residues are in red type. Residue numbering and secondary structure for mouse Skap-hom are indicated above the alignment. DM and PH domain borders are delineated by brackets. Dashed lines indicate disordered regions in the crystal structure. Blue triangles below the alignment mark Skap-hom residues involved in the dimer interface, black ovals indicate

residues in the interface between the DM and PH domains, and black squares mark PH domain residues implicated in lipid head group interaction. PDB entries 1U5D (Skap55), 1H10 (Akt1), 1FAO (Dapp1), 1FGY (Grp1), 1BTK (Btk), and 1W1D (Pdk-1) were used to align PH domain structures. (C) Ribbon diagram of the dimeric DM-PH structure of Skap-hom. The view in the upper panel is along the approximate 2-fold axis of symmetry of the four-helical bundle (top view) and the lower panel is a perpendicular view (front view). The two PH domains are shown in red and yellow, the dimerization domain of one subunit is shown in blue and the other in green. The side chains of Lys125, Arg140 and Tyr151 are shown in stick form to mark the location of the phosphoinositide binding pocket (see Figure 3C).

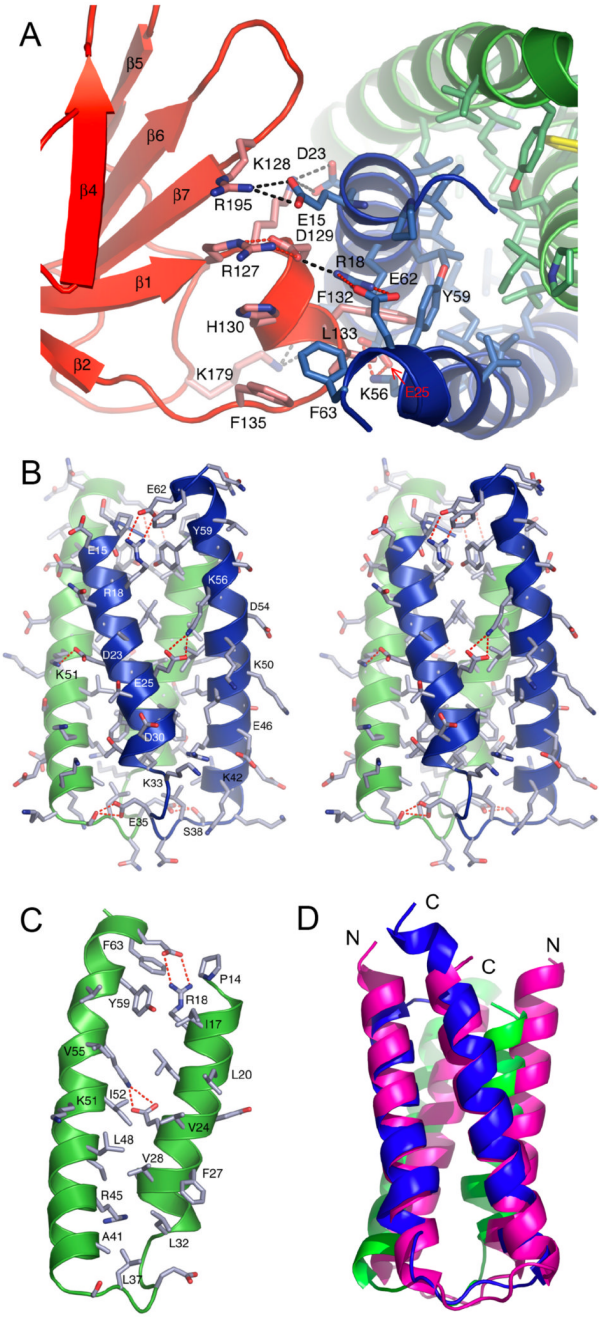

Figure 2.

Interface between the Skap-hom PH and DM domains. (A) The PH domain is shown in red and the DM domain in blue and green as in Figure 1C. Salt-bridges are indicated by dashed lines. Note the helical conformation of the β1-β2 loop (residues Arg127 – Phe135) and the insertion of PH domain residues Phe132 and Leu133 into a hydrophobic pocket on the DM domain. (B) Stereo representation of the DM domain showing the side chains of all residues, with salt-bridges highlighted. Representative charged residues are labeled. (C) View of one subunit of the DM domain showing the hydrophobic and charged residues in the dimerization interface. (D) Superposition of the Skap-hom DM (green and blue) and the dimerization domain

of Nuclear Export Protein Nep/Ns2 of Influenza A (magenta) (Akarsu et al., 2003), which shares a similar overall topology but no clear sequence relationship.

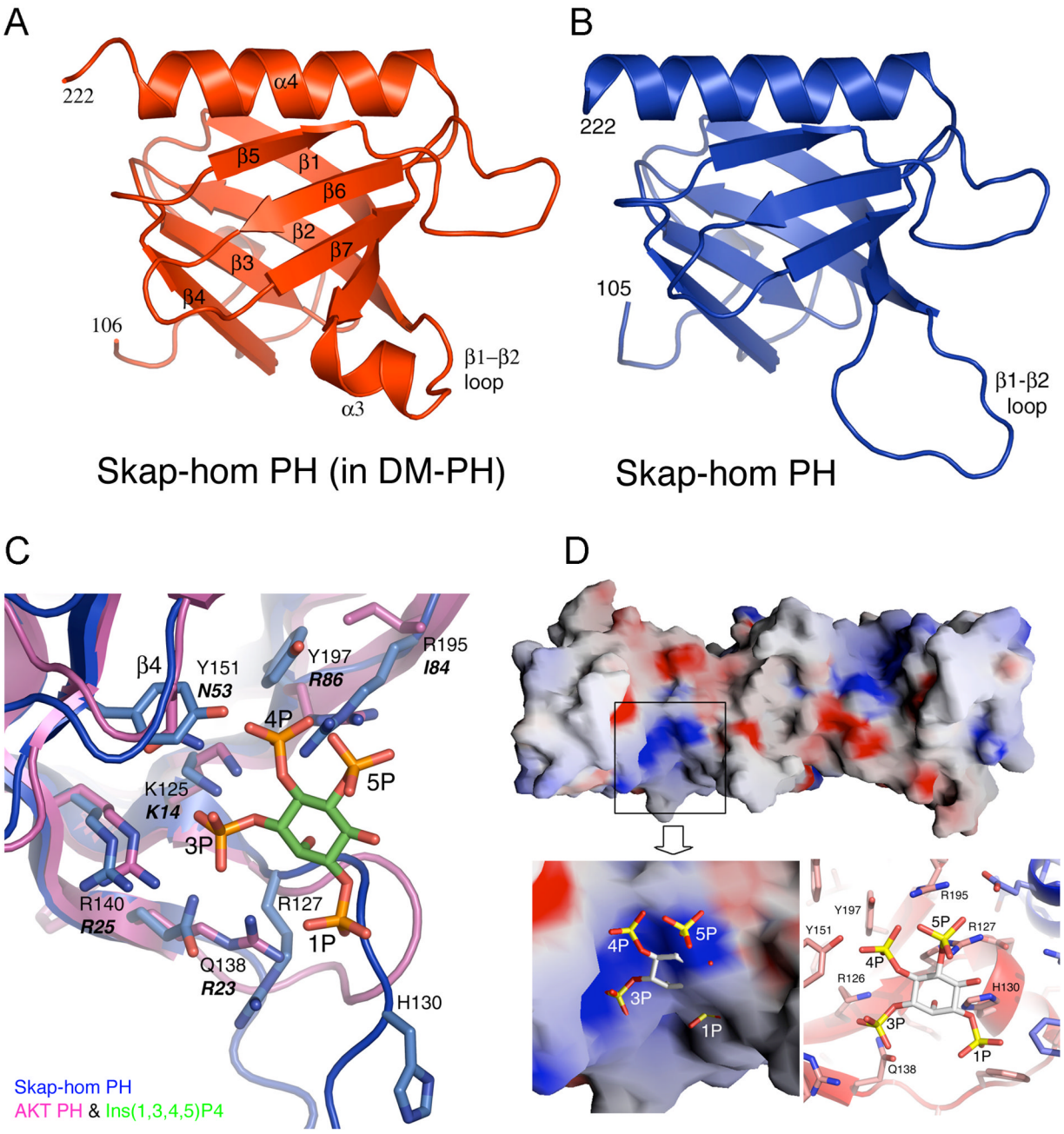

Figure 3.

Comparison of the isolated Skap-hom PH and DM-PH structures. (A) Ribbon diagram showing one of the PH domains in the DM-PH structure. (B) Isolated Skap-hom PH domain. Note the marked difference in conformation of the β1–β2 loop. The helical conformation (α3) seen in the DM-PH structure is incompatible with phosphoinositide binding (see text). Superposition of the Skap-hom PH domain (blue) shown in (C) with the Akt PH domain (magenta) complexed with Ins[1,3,4,5]P_4. Akt residues involved in phosphoinositide binding are labeled in bold italic type; the corresponding residues in Skap-hom are in regular type. (C) Electrostatic surface representation of the dimeric DM-PH structure and close-up of one lipid-binding pocket. The highly basic surfaces (shaded blue) of the phosphoinositide binding pockets are on opposite

faces of the dimer and are recessed relative to the DM domain. The expected position of the head group is modeled into one of the PH domains (inset), based on superposition of the Akt PH domain complexed with Ins[1,3,4,5]P_4. Note the obvious steric clash with the head group due to the helical conformation of the β1–β2 loop.

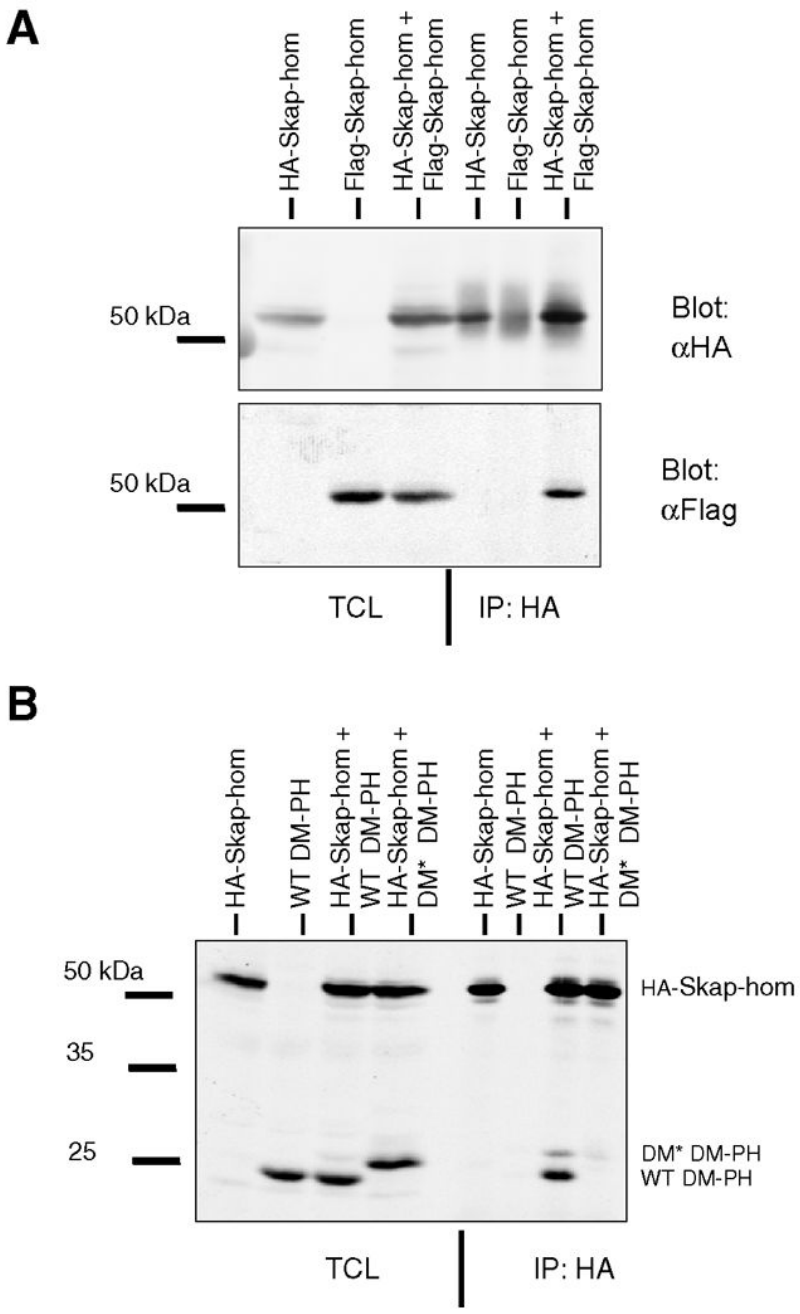

Figure 4.

Skap-hom can homodimerize. (A) Full-length Skap-hom constructs, epitope-tagged with either Flag or HA, were expressed in 293T cells. Total cell lysates (TCL) and anti-HA immunoprecipitates (IP) probed with anti-HA (upper) or anti-Flag (lower) antibodies are shown. The diffuse band present in the anti-HA blots is the 12CA5 heavy chain used for immune precipitation. (B) HA-tagged full-length Skap-hom was expressed with either wild type (WT) or a dimerization domain mutant (DM*) DM-PH fragment and immunoprecipitated with anti-HA antibodies. The resulting immunoblot was probed with anti-Skap-hom antibodies. The upper bands are HA-Skap-hom and the lower bands are the DM-PH, respectively.

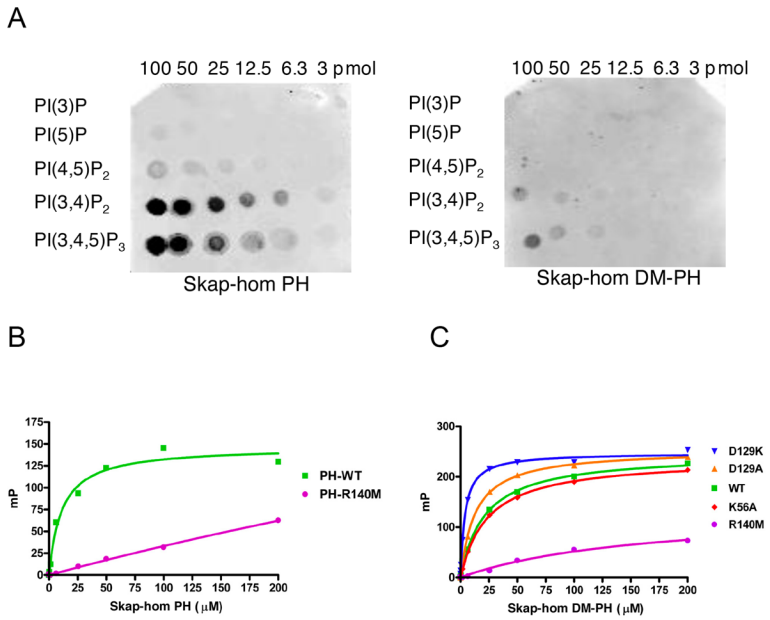

Figure 5.

Phosphoinositide binding of the Skap-Hom PH and DM-PH fragments.. (A) Dot blot assays of Skap-hom PH and DM-PH fragments with the indicated phosphoinositides. (B) Florescence polarization-based binding assays of the isolated Skap-hom PH domain and its R140M mutant to PI[3,4,5]P_3. (C) Florescence polarization-based binding assays of the WT Skap-hom DM-PH fragment and its mutants (D129K, D129A, K56A, R140M) with PI[3,4,5]P_3.

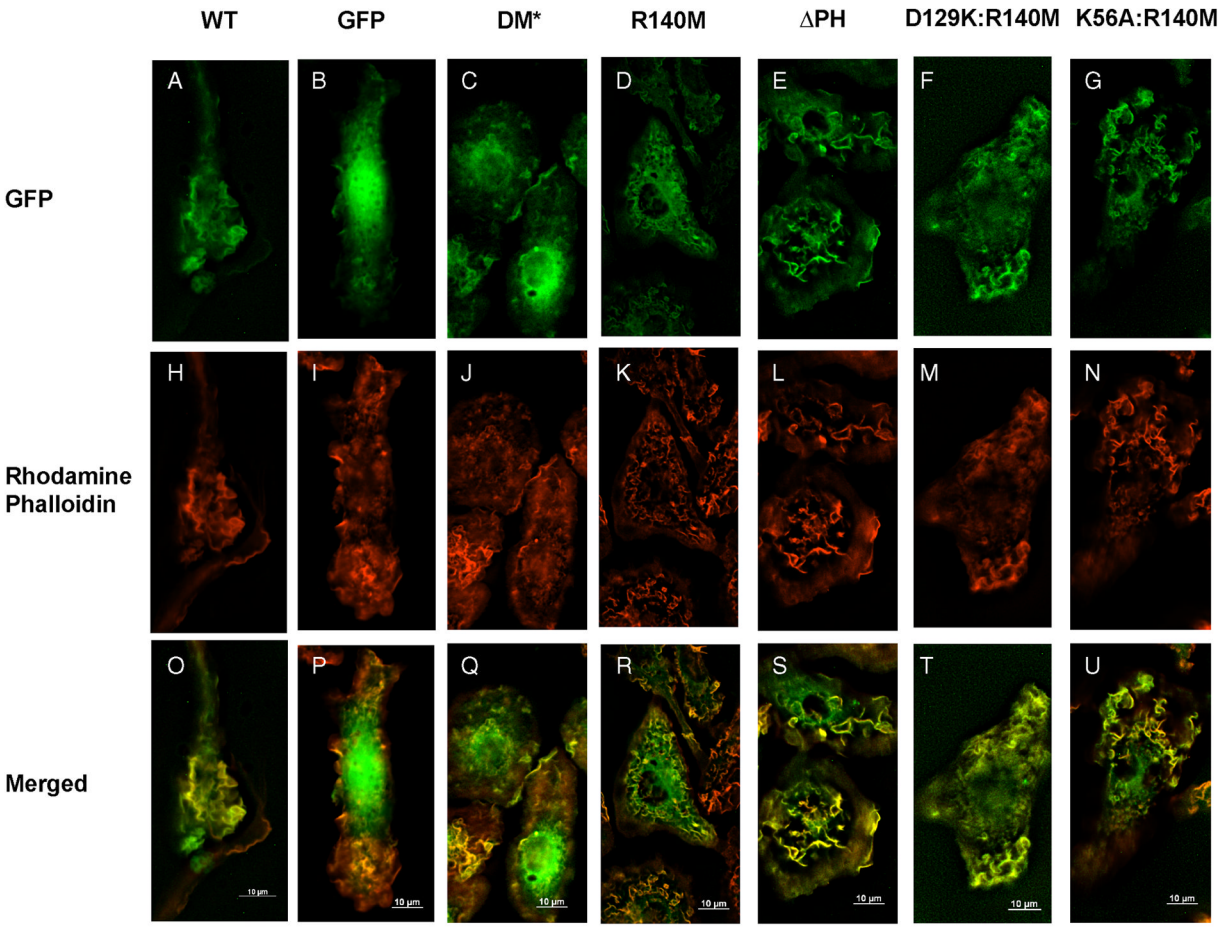

Figure 6.

Localization of GFP-tagged Skap-hom variants in Skap-hom$^{-/-}$ bone marrow-derived macrophages (BMM). Skap-hom$^{-/-}$ BMM were reconstituted with (A) GFP-tagged WT Skap-hom, (B) GFP alone, or (C–G) the indicated GFP-tagged variants of Skap-hom. (H–N) Cells were fixed and counter-stained with rhodamine-labeled phalloidin to visualize the actin cytoskeleton. (O–U) Merged GFP and Rhodamine channels for each infection. WT Skap-hom (A, H and O) co-localizes with actin-rich ruffles. The DM* dimerization domain triple mutant (panels C, J and Q) and the R140M PH domain mutant (panels D, K and R) are diffusely localized. Deletion of the PH domain (ΔPH; E, L and S) results in a protein that localizes to actin ruffles. Skap-hom bearing both the R140M and either the D129K (D129K:R140M panels F, M, T) or the K56A (K56A:R140M panels G, N and U) mutations co-localize with actin-ruffles.

Table 1

Crystal and structure determination statistics.

	SKAP-Hom PH (101–222)	SKAP-Hom DM-PH (14–222)
Wavelength (Å)	1.5418	0.976
Space Group	$P2_12_12_1$	C2
Cell Dimensions a, b, c (Å)	59.8 66.0 144.3	106.2 56.8 89.2
α, β, γ (°)	90.0 90.0 90.0	90.0 95.8 90.0
Molecules/ASU	4	2
Resolution (Å)	25-2.1 (2.15-2.10)	35-2.6(2.67-2.60)
R_{merge} [a]	0.05 (0.38)	0.06 (0.34)
I/σI	16.3 (2.9)	11.9 (2.0)
Completeness (%)	99.4(84.7)	98.7(97.4)
Redundancy	7.5	7.8
No. unique reflections	31,477	15,738
Refinement resolution (Å)	25-2.1	35-2.6
R_{work}/R_{free} [b]	21.3/27.1	17.9/21.6
No. of protein atoms	4,091	2,807
Residue range (chain)	105-219 (a); 105-222 (b) 105-222 (c); 105-219 (d)	12-64; 106-222 (a) 14-64; 106-222 (b)
No. of solvent (H_2O)	213	23
B-factors: Protein (overall)	46.0	60.0
(chains)	56.9 (a); 35.8 (b) 32.9 (b); 61.8 (d)	58.9 (a) 62.5 (b)
Water	44.5	67.4
RMSD Bond lengths (Å)	0.034	0.050
Bond angles (°)	2.337	3.200

Values in parentheses are from the highest resolution shell.

[a] Rsym = 100 × Σ|I − <I>|/Σ<I>, where I is the observed intensity and <I> is the average intensity from multiple observations of symmetry-related reflections.

[b] Rfree was calculated with 5% of the data.